# Mixer Musings and the KISS Mixer

by

Chris Trask / N7ZWY
Sonoran Radio Research
P.O. Box 25240
Tempe, AZ 85285-5240

Email: christrask@earthlink.net

17 December 2011
Revised 23 December 2011
Revised 22 January 2012
Revised 31 January 2012

## Introduction

Mixers, also known as frequency converters, are to be found in virtually any radio communications system, where they are used as modulators, demodulators, phase detectors, and frequency converters. Many forms of mixers are to be found in the technical literature, but in all the majority of realizations come down to either diode ring or current commutating, the former being found mainly in high-performance radio systems while the latter is highly adaptable to inclusion in integrated circuits.

Diode ring mixers are well known for having conversion losses that are in excess of ideal lossless conversion, and many reasons have been proposed for this characteristic. Here, we will take a detailed look at some investigations into the nonideal aspects of diode mixers, which then lead to the design of a novel double-balanced mixer that closely approximates ideal conversion loss together with low distortion and low cost..

## The Diode Ring Mixer

The essential basics of the diode ring mixer are shown in Fig. 1. The technical literature has a vast amount of information and detailed analysis available, which does not need to be repeated here.

Basically, a local oscillator (LO) signal is applied to a balun, producing equal and opposite voltages that are applied to two points of a diode ring. When of sufficient amplitude, the LO signal causes the diodes to turn on and off in pairs. An input RF signal is applied to a second balun, applying equal and opposite voltages to the remaing two points of the diode ring. The swtching of the diodes by the LO signal effectively “chops” the RF signal, resulting in an output intermediate frequency (IF) signal at the centre tap of the RF balun secondary. Some designs have a second IF port at the centre tap of the LO balun secondary, resulting in a differential pair of output IF signals of equal magnitude and opposite phase. The baluns provide very good isolation between the three ports. The intermodulation (IMD) performance is very sensitive to load mismatches at any of the three ports.

Diode ring mixers have a long history, dating back to the late 1940s, and the effects of transformer imbalance and diode mismatch are well understood. IMD products are a result of diode nonlinearities and mismatch, LO signal asymmetry, and improper loading of the three ports. Regardless of the matching of the diodes, the recovery time ($t_r$) and dynamic resistance ($R_j$) of the diodes are significant factors in IMD performance, the latter of which will be discussed in some detail later.

When Schottky barrier diodes are used, diode ring mixers typically have a conversion loss in the order of -6.5dB together with a noise figure (NF) of 6.5dB. Class 1 mixers have a

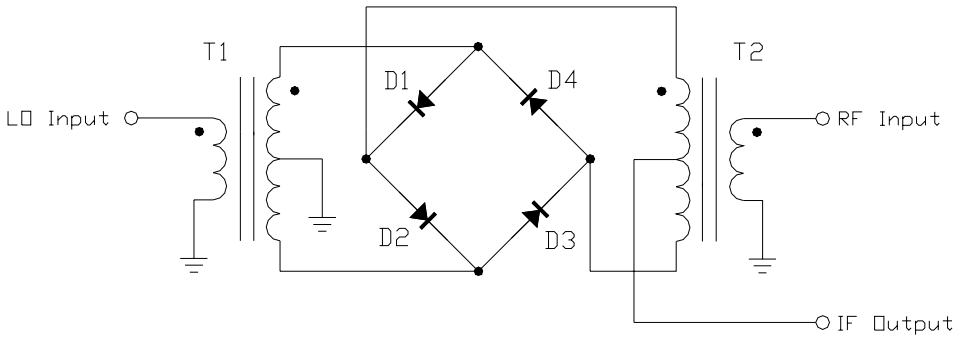


Figure 1 - Diode Ring Mixer

single diode in each arm and generally require an LO power of +7dBm, and thus they are often referred to as “Level 7” mixers. Class 2 mixers, (aka Level 10) have a pair of diodes in series in each arm, and generally require +10dBm of LO power. Class 3 mixers (aka Level 13) have three diodes in series in each arm and require +13dBm of LO power. These forms of diode ring mixers have increasing IMD performance, and still other forms of diode ring mixers include small resistors in series with the diodes to achieve higher IMD performance.

### What’s All This Dynamic Resistance Stuff, Anyhow?

The use of 1:2CT transformers in the diode ring mixer makes the problem of producing well-balanced signals rudimentary as they can be constructed with trifilar twisted wires on binocular or toroid cores and easily duplicated by those with average skill.

The diodes therefore become the critical item, especially with regard to IMD performance. In the small-signal model of a Schottky diode shown in Fig. 2, $R_s$ is the diode series (bulk) resistance, $L_p$ is the package inductance, $C_p$ is the package capacitance, $R_j$ is the diode dynamic (junction) resistance, and $C_j$ is the diode junction capacitance. These last two items are nonlinear, and the diode junction resistance $R_j$ is the primary source of IMD performance degredation. The mean value for $R_j$ can be determined by (1):

$$R_j = \frac{\partial v_a}{\partial i} = \frac{n k T}{q} \frac{1}{I_s \varepsilon^{\frac{q v_a}{n k T}}} = \frac{n k T}{q i} \quad (1)$$

where $v_a$ is the average voltage across the diode junction, $I_S$ is the reverse saturation current, q is the electronic charge ($1.60219 \times 10^{-19}$ J), k is Boltman’s constant ($1.380622 \times 10^{-23}$ J/K), T is the temperature in Kelvin (298.16° at 25°C), and n is an ideality factor ($1 \le n \le 2$).

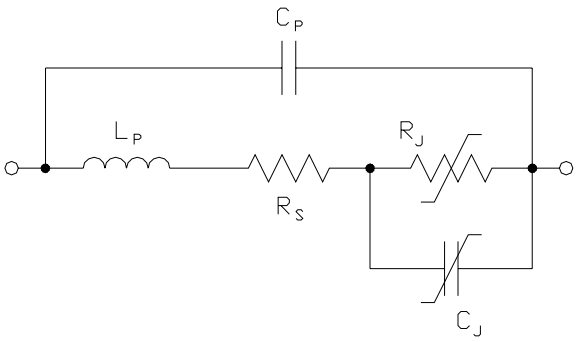


Figure 2 - Small-Signal Model of Schottky Mixer Diode

By inspection of the diode model of Fig. 2, it can be seen that the effects of the nonlinear junction resistance $R_j$ can be mitigated by increasing the ratio of $R_s/R_j$, which is often done in higher level mixers by including a small fixed resistance in series with the diodes, though this results in slightly higher conversion losses. In most cases, it is sufficient to select diodes where the dynamic resistance is a known small quantity and which is controlled in the fabrication process.

The nonlinear junction capacitance $C_j$ is less critical in the overall IMD issue, and it can be determined by way of (1):

$$C_j = \frac{C_j(0)}{\left(1 + \frac{v_a}{v_b}\right)^{\frac{1}{n}}} \quad (2)$$

where $C_j(0)$ is the junction capacitance at zero bias and $v_b$ is the voltage across the bulk resistance $R_S$, so that the total voltage v across the diode terminals is (1):

$$v = v_a + v_b \quad (3)$$

The IMD performance of the diode ring mixer is primarily dependent upon the ratio between the diode series resistance $R_s$ and the diode dynamic resistance $R_j$. Other sources of IMD products would include the transformer cores, but this is generally insignificant and can

easily be alleviated by carefully choosing core materials with linear characteristics and in using cores whose dimensions provide a generous cross-section.

Adding fixed resistors in series with the diodes to improve IMD performance is best suited for applications deep within the receiver, but for front-end applications the added conversion loss and subsequent increase in NF is not acceptable.

To provide a baseline for comparison with future experiments, a diode-ring mixer was constructed and tested. The balun transformers were made using four turns of #32 trifilar wire wound through the holes of a Fair-Rite 2843002402 binocular core, the details of which are shown in Fig. 4 (2, 3, 4). It helps to identify the three wires in the trifilar twist as being red, green and neutral. Now, both ends of the neutral wire are separated out to the right to form the primary winding. An opposite pair of red and green wires are joined together to form the centre tap, and the remaining green and red wire ends then become the ends of the secondary winding.

Three types of diodes were evaluated. First was the Philips/NXP BAT-54S (monolithic series-connected pair, two used), where the conversion loss was approximately 3.9dB and the $OIP_3$ was 24.5dBm. Second was the Avago HSMS-2804 (monolithic series-connected pair, two used), where the conversion loss was approximately 4.2dB and the $OIP_3$ was 22dBm. Last was the Avago HSMS-2829 (monolithic cross-over quad), the performance of which was essentialy the same as for the HSMS-2804.

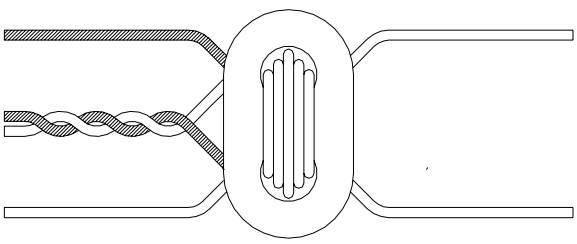

Figure 4 - Balun Transformer Construction Details

The performance of the BAT54S was surprisingly good, approaching the theoretical minimum conversion loss of 3.92dB (5), making this device well-suited for diode mixers up to at least low UHF frequencies The performance for the two HSMS diodes was a bit disappointing, but they are both usable up to low microwave frequencies.

## Diode Embedding Impedances

In most, if not all commercial diode ring mixers, the balun transformers T1 and T2 of Fig. 1 have a convenient impedance ratio of 1:4 (1:2CT turns ratio), giving the secondary terminals an impedance of 100 ohms either side of ground in a 50-ohm system. Each diode therefore sees 200 ohms resistance in series. This is also true for the test mixers described in the previous section.

Diodes such as the Avago HSMS-282 series have a dynamic resistance $R_j$ of 12 ohms and a series resistance $R_s$ of 6 ohms. Although not mentioned in the manufacturer's data sheet, the BAT-54 series must have a slightly lower dynamic and series resistance, owing to the fact that it had better perfromance in the tests described so far. The performance of the three types of diodes tested provide better performance than can be obtained from popular commercial mixers such as the Mini-Circuits SBL-1.

## The Enhanced Diode Ring Mixer

Rather than add resistors in series with the diodes, the resistance seen by the diodes can be readily increased by changing the turns ratio of the balun transformers T1 and T2. Doing so, however, will affect the IF source impedance of T2, and this must be taken into consideration. With a turns ratio of 1:4CT, the diodes will see a series resistance of 800 ohms and the IF source impedance will be 200 ohms, the

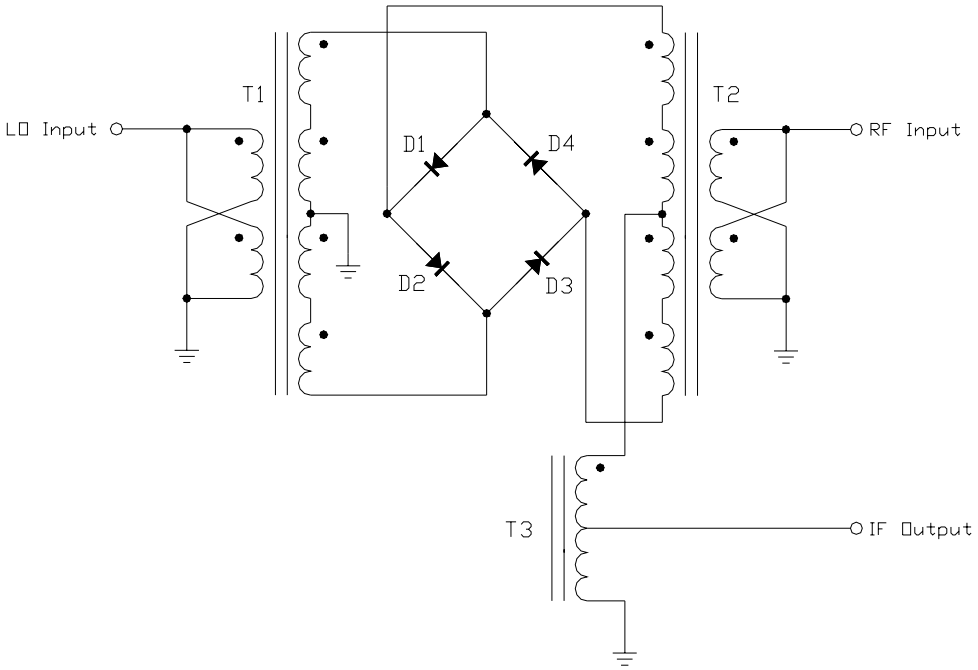


Figure 5 - Enhanced Diode Ring Mixer

latter of which can easily be accomodated by adding a 1:2 unun autotransformer, as shown in Fig. 5.

A commercial 1:4CT transformer such as the Mini-Circuits T16-6T could be used for T1 and T2, however they are not exceptionally good performers in terms of loss and bandwidth. As shown in Fig. 6, a much better performing transformer can be obtained by way of an interesting configuration in which a pair of trifilar windings on a binocular core are interconnected in such a way as to provide very good coupling, balance, and bandwidth.

Construction consists of two windings of four turns of #32 trifilar wire along the outside and through the holes of a Fair-Rite 2843002402 binocular core, the details of which are shown in Fig. 6 (2, 3, 4). As with the earlier discussion of transformer construction, it helps to identify the three wires in the trifilar twist as being red, green and neutral. Again identifying the three wires in the trifilar twist as being red, green and neutral, at one end of the core the two red wires are joined together, and then the two green wires are joined together.

At the second end of the core, an opposite pair of red and green wires are joined together, forming the centre tap of the secondary winding. The remaining opposite red and green wires are the end terminals of the secondary winding. The neutral wires are crossed over

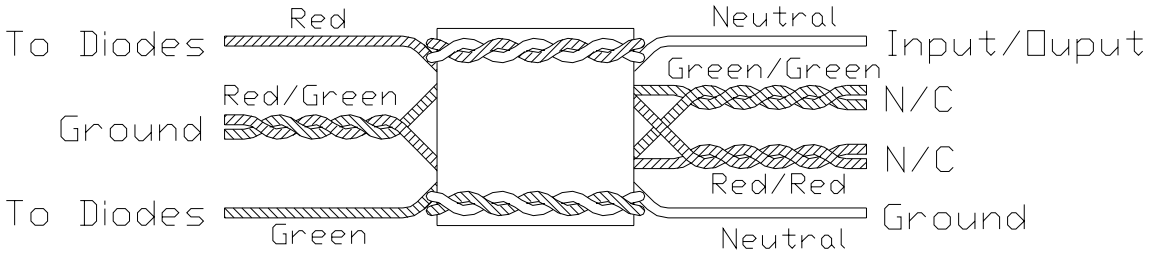


Figure 6 - Construction Details for Transformers T1 and T2

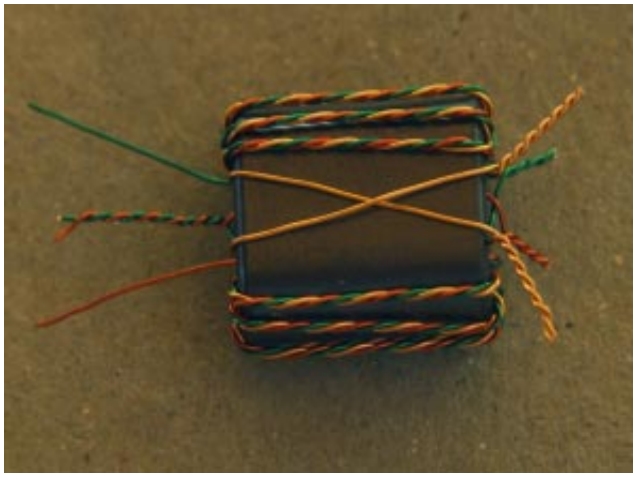

Figure 7 - Contruction Detatils
for Transformers T1 dnd T2

along the bottom surface to the opposite ends of the neutral wires on the first end of the core, effectively connecting the two windings in parallel to form the primary winding, as shown in Fig. 5. The photograph of Fig. 7 shows the construction of this transformer in detail.

The 1:2 unun autotransformer was made by winding four turns of #32 bifilar wire through the holes of a Fair-Rite 2843002402 binocular core, the details of which are shown in Fig. 8 (2, 3, 4). Identifying the two wires in the bifilar twist as being red and green, an opposite pair of red and green wires are joined together to form the output centre tap, and the remaining green and red wire ends then become the input and ground terminals.

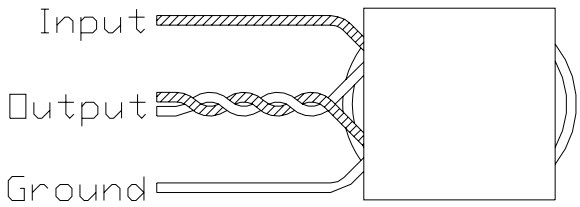


Figure 8 - Contruction Detatils
for Transformer T3

Testing with both the BAT-54S and HSMS-2804 diodes showed that the conversion loss remained fairly much the same, but the $OIP_3$ deteriorated by about 3dB, which may be attributed to the higher signal voltages across the diodes. No further testing was deemed to be worthwhile so the test circuit was set aside.

**The Split-Ring Mixer**

It has been of considerable interest to determine if the difference between the turn-on ($t_{on}$) and turn-off ($t_{off}$) times of the diodes affects the conversion loss and/or the IMD performance. To do this, the diode ring of Fig. 1 was broken into two series pairs and an additional LO balun transformer was added. Shown in Fig. 9, this mixer was dubbed the “Split-Ring Mixer”.

Initial testing with BAT-54S diodes

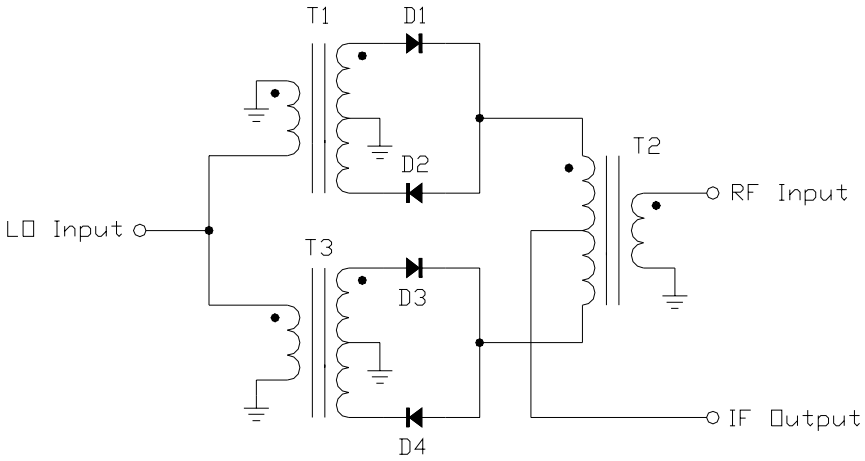


Figure 9 - Split-Ring Mixer

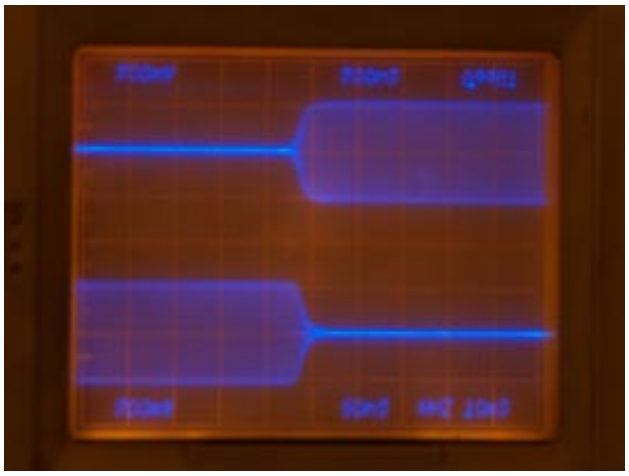

Figure 10 - Split-Ring Mixer Timing

showed that the split-ring mixer of Fig. 9 has a conversion loss of 3.9dB, essentially the same as measured for the conventional diode ring mixer of Fig. 1 using the same diode. The IMD performance was also the same. Similar results were observed when using the HSMS-2804 diodes.

The switching characteristics of the two diode pairs were evaluated for the BAT-54S diodes by measuring the signal voltages at the junctions of D1/D2 and D3/D4. Shown in Fig. 10, the two traces have no signal present when the diodes are turned ON (conducting) and signal present when they are turned OFF (nonconducting). Comparing the two traces, it can readily be seen that the diodes turn OFF faster than they turn ON by about 20nSec, the opposite of what would be expected.

### The Compensated Split-Ring Mixer

Although we take great care to ensure that LO signals are symmetrical, such as 50% duty cycle square waves, the test results shown here indicate that close attention to such details may be in vain. SInce the diodes in this test turn OFF faster than they turn ON, the actual switching duty cycle is less than 50%. Therefore the diode switching time is less than 50%, resulting in a short time period in which all four diodes are OFF.

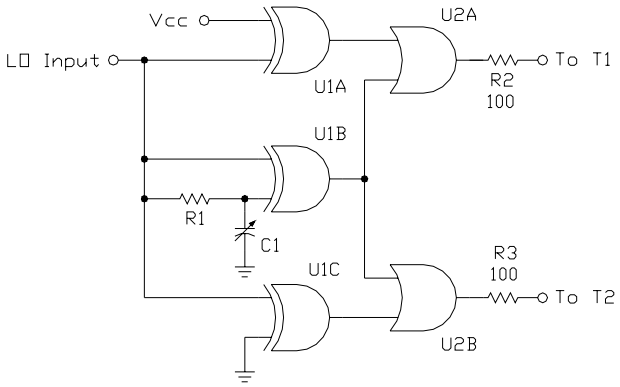


Figure11 - Variable Duty Cycle LO Driver

To evaluate the consequences of the non-ideal switching characteristics of the diodes, a logic circuit providing dual tracking outputs with variable duty cycles was constructed, shown in Fig. 11. By varying the LO duty cycle, the diode switching was corrected to 50%. The overall improvement was not sufficient to warrant such complexity and added cost. In addition, the use of logic circuity would limit the use of the split ring mixer to frequencies below VHF, similar to what limits the useage of the H-Mode mixer.

To more properly compensate for the different $t_{on}$ and $t_{off}$ times an additional pair of BAT-54S diodes was added between the LO input terminal and the primary windings of T1 and T3, as shown in Fig. 12, and the topology is referred to here as the compensated split-ring mier. With an applied LO square wave having a 50% duty cycle, diode D5 provides an LO signal of less than 50% to the primary winding of transformer T1. If the switching times of diode D5 are the same as those of diodes D1/D2, then the result is a 50% switching time. Similarly, diode D6 provides an LO signal of more than 50% duty cycle to the primary winding of transfomer T3, resulting in a 50% switching time for diodes D3 and D4.

Capacitor C1 is added in order that any DC component in the LO signal does not disturb the switching characteristics of diodes D5/D6, such as would be present from genera-

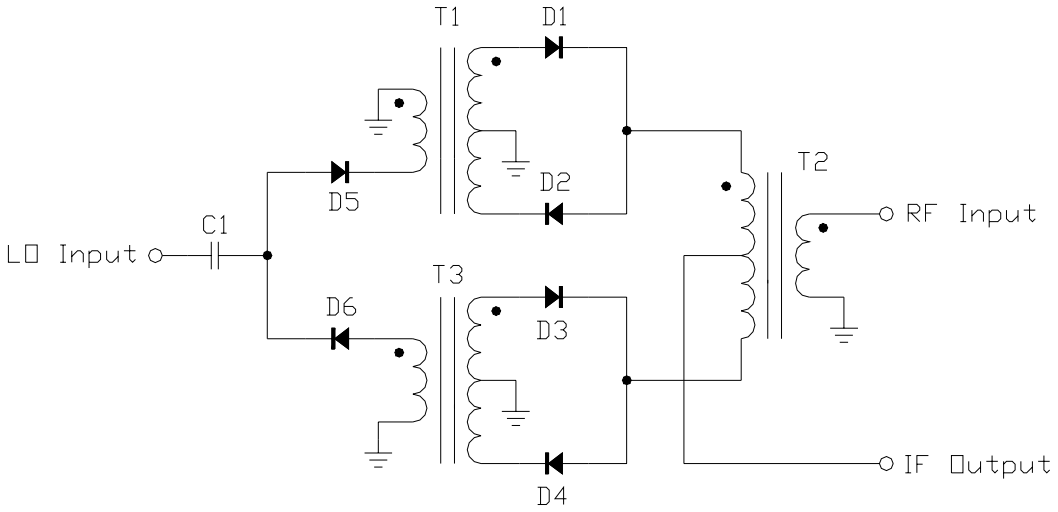


Figure 12 - Compensated Split-Ring Mixer

tors having digital output signals without offset capability.

The result of adding the switching compensation diodes D5/D6 is shown in Fig. 13. Here it can be seen that diodes D1/D2 turn OFF at almost the exact same time that diodes D3/D4 turn ON. As shown in Fig. 13, the time discrepancy is corrected to less than 2nSec. However, just as with the earlier test using the time-correcting logic circuit of Fig. 11, there was little if any improvement in the conversion loss or IMD performance, so this test circuit was also set aside.

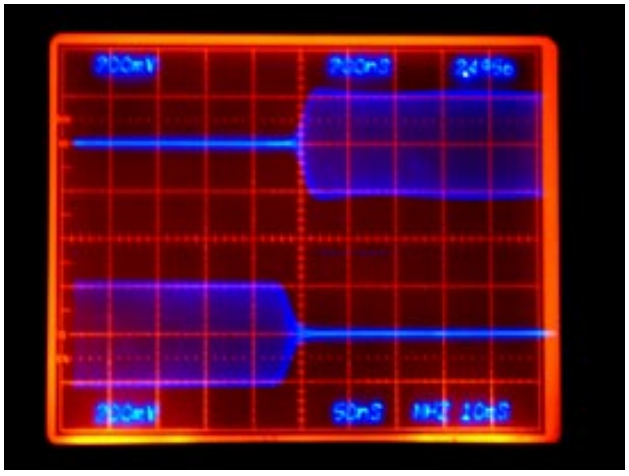

Figure 13 - Compensated Split-Ring Mixer Timing

### The KISS Mixer

Examining the split-ring mixer schematic of Fig. 9 revealed that the LO balun transformer T1 and diodes D1/D2 formed a switch to ground that is turned ON during the negative half of the LO signal, while balun transformer T3 and diodes D3/D4 formed an identical switch that was turned ON during the positive half the LO signal. A functional diagram of this is shown in Fig. 14.

The switches of Fig. 14 can be easily realized by way of a monolithic SPDT switch, such as the Fairchild FSA3157. By adding a few

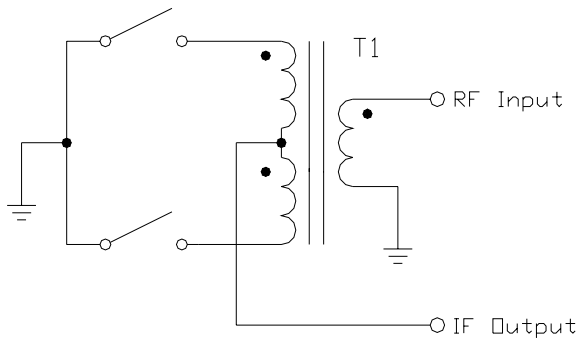


Figure 14 - Split Ring Mixer Functional Diagram

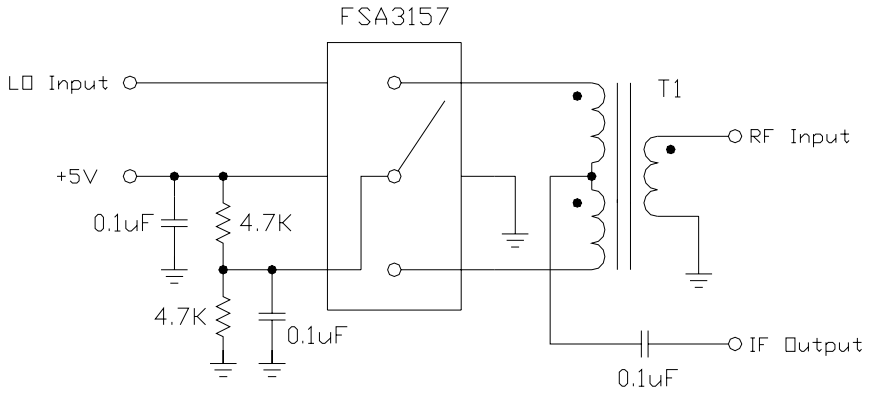


Figure 15 - The KISS Mixer

passive components, a vey simple mixer can easily be realized, as shown in Fig. 15, and this simplicity prompted the name KISS (an American acronym meaning Keep It Simple, Stupid) Mixer. Since the DC voltage at the switch input teminal and the switch output terminals is the same, no LO current will flow through the primary or secondary windings, thus isolating the LO signal from the IF and RF signal terminals. The KISS mixer therefore has similar LO, IF, and RF isolation properties as does a diodering mixer, and the IF and RF terminals can be interchanged.

In order to ensure that the LO signal has fast rise and fall times, a pulse shaping circuit such as that shown in Fig. 16 may be employed. The two inverters U1A and U1B may be those of the Fairchild NC7WZ04, which has power supply requirements similar to those of the FSA3157.

The pulse shaper circuit of Fig. 16 assumes that the input signal is a 50% duty cycle square wave and that the switchin threshold of the inverters is at Vcc/2. Neither of these assumptions is valid in the broad sense as many LO signal sources are sine waves. In addition, threshold voltages for HCMOS logic can vary considerably, and they are not constant over temperature.

In a variation of the variable duty cycle LO driver of Fig. 11, the LO driver of Fig. 17 uses a differential integrator in a feedback loop that automatically adjusts the threshld point to ensure a 50% duty cycle. The theory here is quite simple. If the two exclusive-NOR (XNOR) gates U1A and U1B are a matched monolithic pair, then their input threshold voltages and their output high and low voltages will be the same. U1A is used as an inverter and U1B is used as a buffer.

Now, the average DC voltage of the two outputs will be the same when both output voltages have the same duty cycle, which may vary slightly from 50% if the rise and fall times

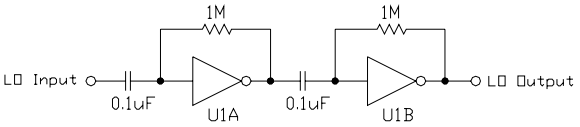


Figure 16 - LO Pulse Shaper

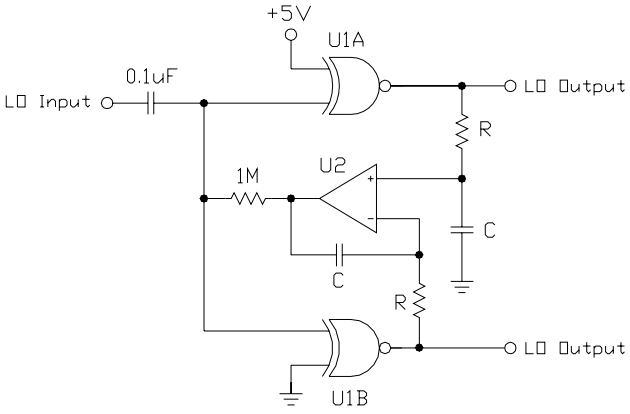


Figure 17 - 50% Duty Cycle LO Pulse Shaper

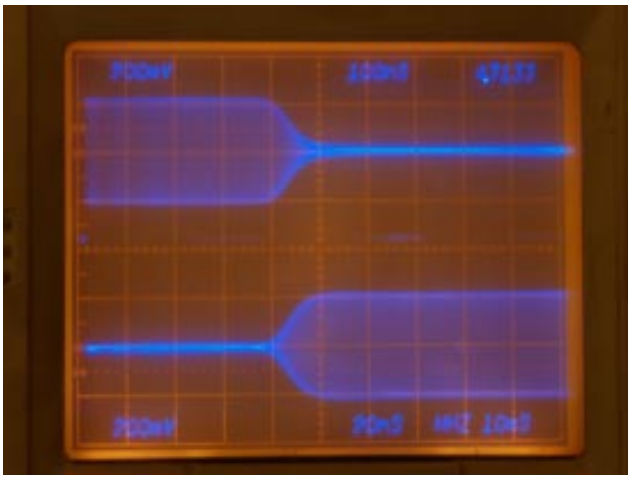

Figure 18 - KISS Mixer Timing

are different.

Opamp U2 is used as a differential integrator, comparing the two output average voltages and applying an offset to the inputs of U1A and U1B. Resistors R and capacitors C determine the time constant of the integrator. Opamp U2 can be a low frequency rail-to-rail device such as the Texas Instruments LMV321.

**Preliminary Test Results**

Preliminary testing shows that the KISS Mixer of Fig. 15 has about 3.9dB of conversion loss at low frequencies and does not show any significant increase until above 100MHz, Further testing shows that the KISS Mixer has an $OIP_3$ of at least +40dBm, tapering off to

Table 2 - SPDT Switches
Suitable for the KISS Mixer

| Switch | $R_{on}$ ohms | $t_{on}$ nSec | $t_{off}$ nSec | $C_{off}$ pF | $f_{max}$ MHz |
|---|---|---|---|---|---|
| FSA3157 | 7.0 | 3.4 | 2.1 | 6.5 | 250 |
| DG3157 | 9.0 | 2.9 | 2.9 | 6.5 | 250 |
| DG2307 | 9.0 | 2.9 | 2.9 | 6.5 | 250 |
| PI5A124 | 7.2 | 7.0 | 1.0 | 5.5 | 326 |
| PI5A3157 | 5.0 | 3.4 | 2.1 | 6.5 | 250 |
| PI5A4599A | 7.0 | 7.0 | 1.0 | 5.0 | 300 |
| TS5A63157 | 4.0 | 3.4 | 2.8 | 5.0 | 371 |

Table 1 - KISS Mixer Performance Data (FSA3157)

| RF Freq (MHz) | Conversion Loss (dB) | $OIP_3$ (dBm) |
|---|---|---|
| 1.0 | -3.9 | >+40.0 |
| 2.0 | -3.9 | >+40.0 |
| 5.0 | -3.9 | >+40.0 |
| 10.0 | -3.9 | >+40.0 |
| 15.0 | -3.9 | |
| 20.0 | -4.0 | >+35.0 |
| 25.0 | -4.0 | |
| 30.0 | -4.0 | >+35.0 |
| 40.0 | -4.0 | |
| 50.0 | -4.0 | +29.0 |
| 60.0 | -4.0 | |
| 70.0 | -4.0 | |
| 80.0 | -4.0 | |
| 90.0 | -4.1 | |
| 100.0 | -4.5 | |
| 110.0 | -5.2 | |

+29dBm at 50MHz. The measurement of $OIP_3$ was made difficult due to the dynamic range of the HP141T spectrum analyzer being used.

As with the earlier split-ring mixer, the switching characteristics of the FSA3157 were evaluated. The results are shown in Fig. 18, revealing that the 50% points are less than 5nSec apart. The manufacturer's datasheet states that the "break-before-make" time ($t_{BMM}$) is in the order of 0.5nSec.

There are many devices that are suitable for use in the KISS mixer, most of which have $t_{BMM}$ times similar to that of the FSA3157 used here, including the TS5A63157, which has very attractive $R_{on}$ and $f_{max}$ performance.

A few combinations of SPDT switches and transformers were evaluated. Overall, the FSA3157 gave the best IMD performance, and when combined with a transformer constructed with a Fair-Rite 2861002402 binocular core the conversion loss is 4dB or better to at least

60 MHz.

When combined with a transformer constructed with a MicroMetals BLN1728-8 binocular core, the TS5A63157 gives good conversion loss to about 150 MHz, beyond which the switching speed of the logic becomes a serious obstacle. IMD performance though is in the order of +30dBm to +35dBm $OIP_3$.

### It's Déjà Vu All Over Again

A little bit ot techno-archaeology reveals that the basic topology of the KISS Mixer is not entirely novel, having been originaly described by Squires in US Patent 3,383,601 in 1968 (6). More refined versions were later patented by Sharma and Sosin in 1990 (7) as well as by Dobrovolny in 1991 (8). The topology also appears in two textbooks related to radio design (9,10)

In the last of these, a KISS Mixer is described that makes use of a pair of NEC NE868299 mcrowave FETs. It is stated in the accomanying text that an intercept point of +30dBm can be obtained with an LO injection power of well under 1W, but that the balance of such a mixer making use of discrete transistors will be poorer than the balance of a diode mixer because of the difficulty of matching the rather complex transistor parameters over the operating range (10). At that time, comparable performance could be obtained from diode mixers at the cost of higher LO injection levels. These obstacles undoubtedly caused the KISS mixer to be less than attractive, so the interest in the topology diminished and was all but forgotten.

The advent of monolithic quad arrays of switching MOSFETs, bus switches, video switches, and other devices since that time has changed the opportunity for realizing good performance from the simple KISS Mixer topology.

### Circuit Refinements

Dobrovolny (8) initially uses a KISS Mixer as an opportunity to incorporate one or two matching networks that absorb the parasitic capacitances of the switching devices as well as parasitics of the transformer, resulting in an extension of the high frequency performance. This method is not entirely novel, being used earlier to extend the frequency performance of wideband transformers (11, 12, 13, 14).

To incorporate a simple matching network to extend the high frequency performance, we first examine the small-signal incremental model of the KISS Mixer, as shown in Fig. 19. Here, the loss resistances of the windings and the induced core loss resistance have been omitted as they are insignificant when compared to the source and load resistance as well

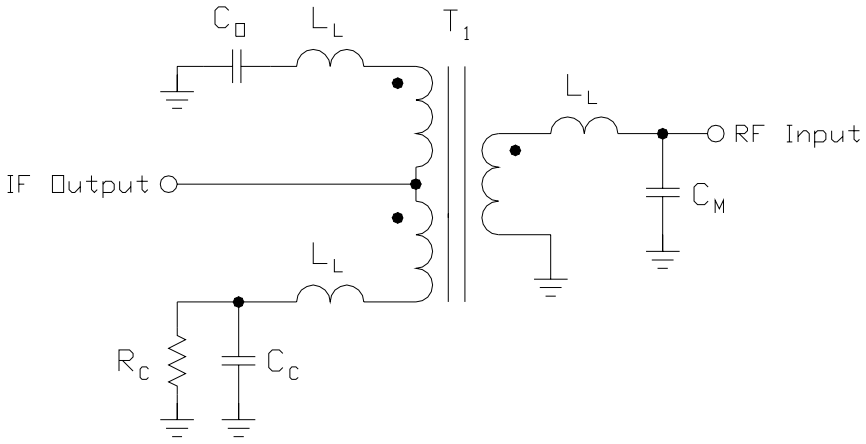


Figure 19 - KISS Mixer Small Signal Incremental Model

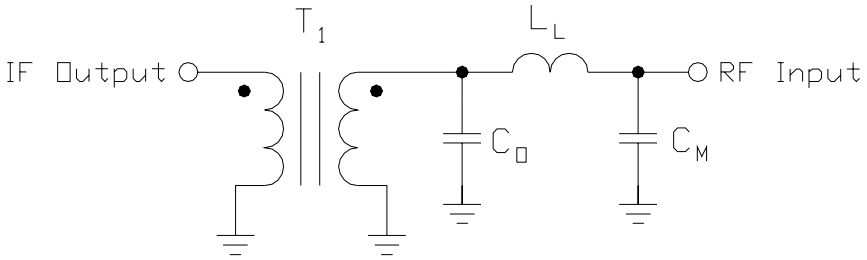


Figure 20 - Simplified KISS Mixer Small Signal Incremental Model

as the series resistance $R_C$ of the closed switch. The interwinding and intrawinding capacitances of the windings have also been omitted as they are insignificant when compared with the closed and open capacitances of the switches, labeled as $C_C$ and $C_O$, respectively.

The inductors labeled $L_L$ represent the leakage inductance of the three windings, and for wideband transformers made with trifilar windings they are generally equal. Although these inductances are fairly small for high-frequency wideband transformers, they will soon play an important rôle in the design process.

The model of Fig. 19 is now further simplified, as shown in Fig. 20. Here, the switch parasitic elements $R_C$ and $C_C$ have been removed as they are relatively insignificant. The two leakage inductances on the secondary side have also been removed as hey have little effect within te passband. Finally, the open switch capacitance $C_O$ is transposed to the pimary side of $T_1$, leaving us with a 1:1 ideal transfomer and a 3-pole lowpass filter network.

PSpice analysis of the model of Fig. 19 reveals that the model elements removed to facilitate the simplified model of Fig. 20 have a noticable effect on the transition band of the 3-pole matching network, making the realization of anything other than a Butterworth (maximally flat passband) response difficult, if not impractical.. To begin the design process, we first recognize that the open switch capacitance $C_O$ is the driving design parameter which determines the maximum operating frequency by way of:

$$\omega_{max} = \frac{1}{C_O R_S} \tag{4}$$

where $R_S$ is the RF source resistance. From this, the matching capacitance $C_M$ is determined by way of:

$$C_M = C_O \tag{5}$$

The leakage inductance $L_L$ now becomes a design parameter of transformer $T_1$, and is determined by way of:

$$L_L = \frac{2 R_S}{\omega_{max}} \tag{6}$$

where $\omega_{max}$ is from Eq. 4. Achieving the required leakage inductance places demands on the design of transformer $T_1$, and in some instances the angular length of the wire will constitute a portion of the leakage inductance.

According to PSpice analysis, incorporation of a Butterworth matching section with the FSA3157 SPDT switch results in an improvement of the RF 1dB cutoff frequency from 135MHz to 220MHz.

## Prototype Construction

The prototypes tested here were constructed on Ivan board (Circuit Specialists IF-RFB), which can be difficult when working with small SMT parts such as SC-70-6. To alleviate that, a small PCB board design is provided in Appendix A, which includes reverse image 1:1 artwork that can be used with toner

transfer PCB fabrication. In the parts list, C8 is the matching capacitor CM discussed in the previous section. Transformer T1 can be a Mini-Circuits part or can be constructed as discussed herein. Resistor R8 is included to provide a DC source for using the KISS Mixer as a zero-IF demodulator.

**And In This Corner...**

One of the more interesting entries in the mixer community has been the H-Môde Mixer, originally devised by Colin Horrabin, G3SBI (15). In it's basic form shown in Fig. 21, the H-Mode mixer consists of three 1:2CT balun transformers and four FET switches. Subsequent designs have made use of digital bus switches and other devices.

By having the source terminals of the FET switches grounded, the H-Môde Mixer supposedly has better IMD performance than if the devices were connect as a ring such as the numerous circuits proposed by Ed Oxner of Siliconix (16). It has been a long-term disappointment that the promoters of the H-Mode Mixer have yet to make a detailed comparison of the two topologies so as to demonstrate that

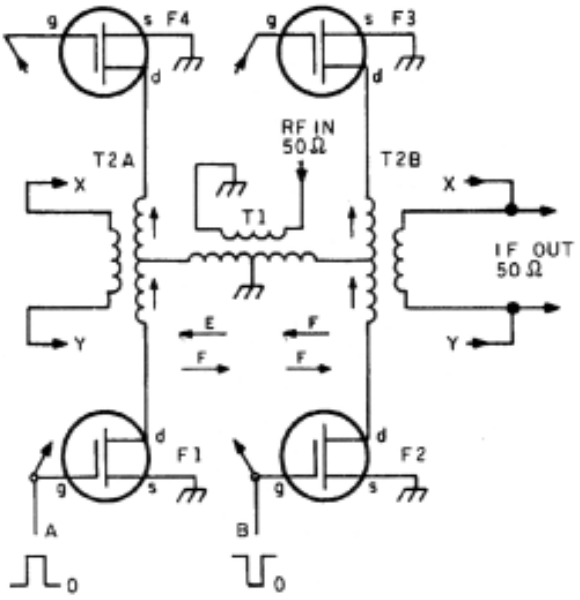


Figure 21 - Basic FET H-Mode Mixer (from reference 6)

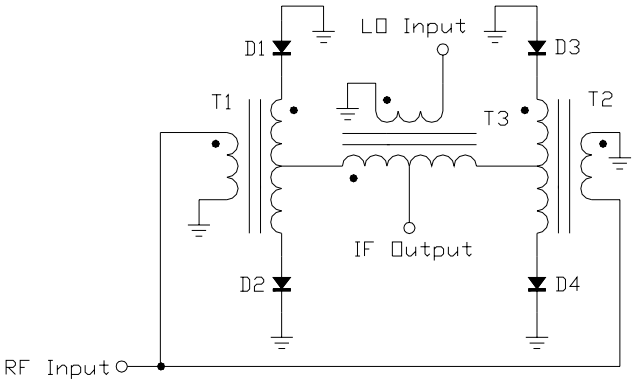


Figure 22 - Diode-Based H-Mode Mixer

the H-Môde topology has performance superior to the FET-ring mixer when made with the exact same parts.

To remedy that omission, a diode-based H-Môde Mixer was constructed, shown in Fig. 22, using the same BAT-54S and HSMS-2804 diodes and transformers as used in the baseline evaluation of the diode ring mixer of Fig. 1. It was found that the conversion loss and IMD performances of the diode ring mixers and the diode-base H-Mode mixers were virtually identical.

One innovative designer, Gennady Bragin, KZ4HK, of the Suntel Corporation in Moscow, began with the H-Môde Mixer of Fig. 21 and reduced it in form, as shown in Fig. 23 (17). The first transformer is a 1:1 current balun, and the second is the familiar Guanella 4:1 balbal impedance transformer. Both transformers are constructed using parallel-wire TLT techniques, which provides good coupling, low insertion loss, and good wideband frequency performance (2, 3, 4).

Each FET switch is actually two in parallel, which helps reduce the switch ON resistance. The performance of this mixer is quite good, virtually equal to many of the H-Môde Mixer realizations, making it a worthy accomplishment.

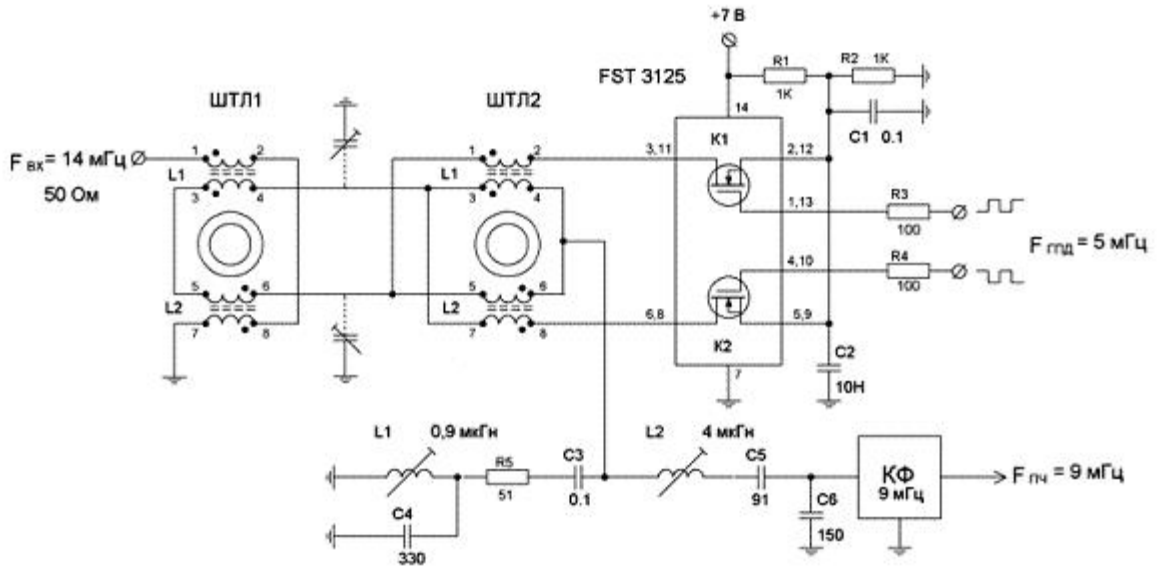


Figure 22 - TLT-Môde Mixer by Gennady Bragin, RZ4HK

At least one designer is not happy with this simplicity and performance, and has elaborated on Bragin's circuit, almost tripling the number of components with little improvement in performance (18).

## Synopsis

The KISS Mixer described herein is a minimum component mixer with performance comparable to that of the better H-Môde Mixer designs. This design evolved from considerable experimentation with diode ring mixer derivatives, and at least one H-Môde Mixer designer is converging on this simple realization.

*We keep making things better, not more expensive* - Howard Cosell

## References


1. Indresaeter, H., *Noise Characterization of an X-Band Hot Carrier Mixer Diode*, MS Thesis, Texas Tech University, Lubbock, Texas, August 1973.
2. Trask, C., "Wideband Transformers: An Intuitive Approach to Models, Characterization and Design," *Applied Microwave & Wireless*, Vol. 13, No. 11, November 2001, pp. 30-41.
3. Trask, C., “Designing Wide-band Transformers for HF and VHF Power Amplifiers,” *QEX*, May/April 2005, pp. 3-15.
4. Walker, John L.B., Daniel P. Meyer, Frederick H. Raab, and Chris Trask, *Classic Works in RF Engineering: Combiners, Couplers, Transformers, and Magnetic Amplifiers*, Artech House, 2006.
5. Tucker, D.G., *Modulators and Frequency-Changers for Amplitude-Modulated Line and Radio Systems*, MacDonald & Co., London, 1953, pp. 74-75.
6. Squires, W.K., *Mixer Circuit Employing Linear Resistive Elements*, US Patent 3,383,601, 14 May 1968.
7. Sharma, Rakesh and Boleslaw M. Sosin, *Mixer*, US Patent 4,977,617, 11 December 1990 (also UK Patent 2210224A, 1 June 1989 and European Patent 0308273A1, 22 March 1989).
8. Dobrovolny, Pierre, *High Level Wide Band RF Mixer*, US Patent 5,027,163, 25 June 1991.
9. Gosling, William (ed), *Radio Receivers*, Peter Peregrinus, Cambridge, England, 1986.
10. Sabin, William E. and Edgar O. Schoenike (eds), *HF Radio Systems & Circuits, 2nd ed.*, Noble Publishing Co., Atlanta, Georgie, 1998.
11. Hilbers, A.H., “High-Frequency Wideband Power Transformers,” *Electronic Applications*, Vol. 30, No. 2, Apr 1971, pp. 64-73.
12. Hilbers, A.H., “Design of High-Frequency Wideband Power Transformers,” *Electronic Applications*, Vol. 32, No. 1, January 1973, later reprinted as Philips Application Note ECO7213.
13. Trask, C., "Wideband Transformers: An Intuitive Approach to Models, Characterization and Design," *Applied Microwave & Wireless*, Vol. 13, No. 11, November 2001, pp. 30-41.
14. Trask, C., *Wideband Transformer Models:Measurement and Calculation of Reactive Elements*, 10 October 2008 (online resource).
15. Hawker, P., “G3SBI’s High Performance Mixer,” *Technical Topics, Radio Communication*, October 1993, pp. 55-56.
16. Oxner, Ed, “Active Double-Balanced Mixers Made Easy with Junction FET’s,” *EDN*, 5 July 1974, pp. 47-53.
17. http://martein.home.xs4all.nl/pa3ake/hmode/tlt-hmode.html
18. Skydan, Oleg, “The ‘True’ TLT H-Mode Mixer,” *QEX*, July/August 2010, pp. 10-15.

## Appendix A

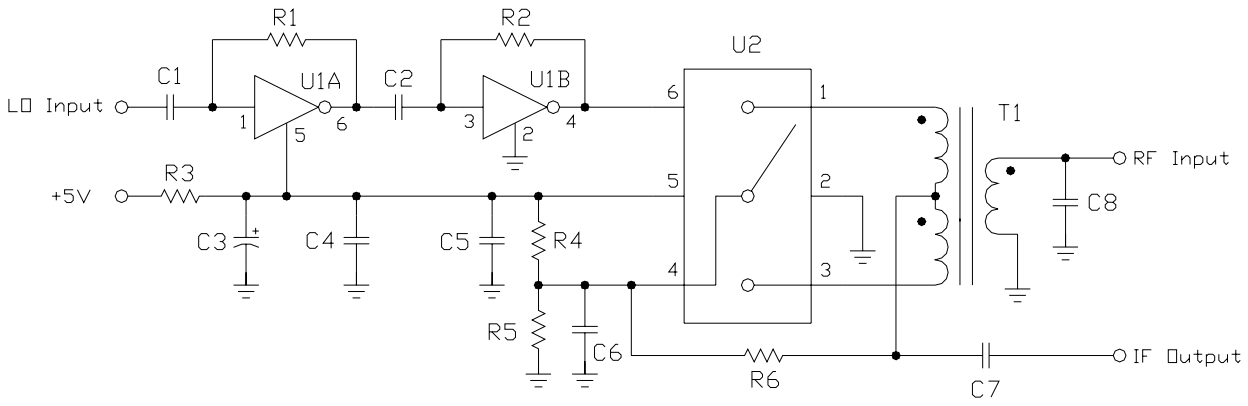


Fig. A1 - KISS SPDT Mixer Schematic

Table A1 - KISS SPDT Mixer Parts List

C1, C2, C4, C5, C6, C7 - 0.1uF 16V (size 0603)
C3 - 10uF 10WVDC (size 1206). Kemet T491A106KO16AT or equivalent
C8 - See text

R1, R2 - 1M (size 0603)
R3 - 100 ohms (size 1206)
R4, R5 - 4.7K (size 0603)
R6 - optional (see text)

T1 - Mini-Circuits T4-6T or handmade (see text)

U1 - Fairchild NC7WZ04 or equivalent
U2 - see text

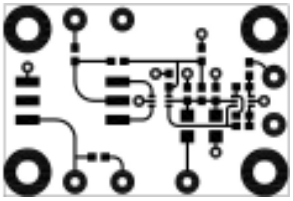

Fig. A2 - KISS SPDTMixer PCB Artwork (reversed)

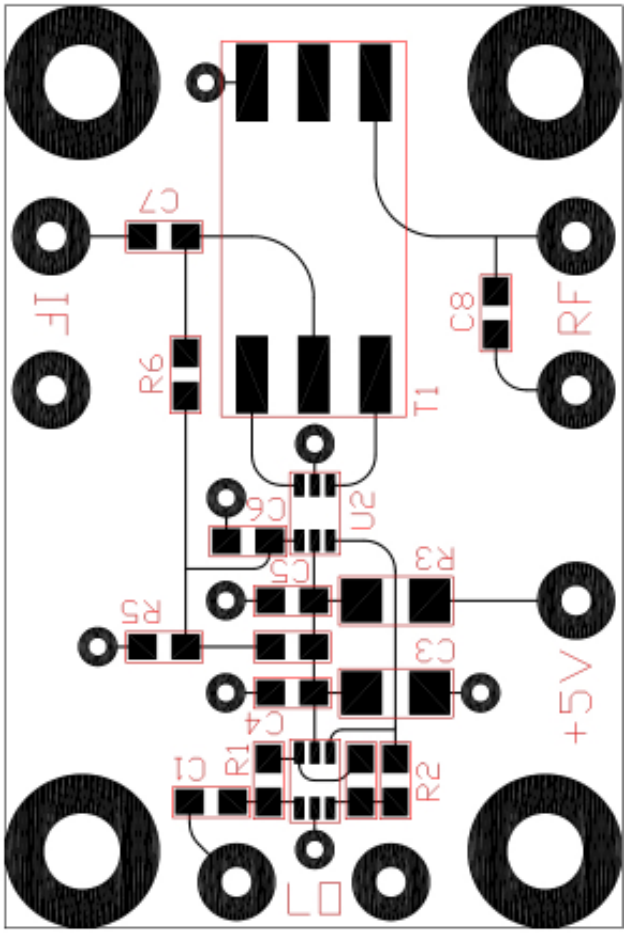


Fig. A3 - KISS SPDTMixer PCB Parts Placement